# Unprecedented Chemical Reactivity of a Paramagnetic Endohedral Metallofullerene La@$C_s$-$C_{82}$ that Leads Hydrogen Addition in the 1,3-Dipolar Cycloaddition Reaction

Yuta Takano,[a] Zdenek Slanina,[b] Jaime Mateos-Gil,[c] Takayoshi Tsuchiya,[d] Hiroki Kurihara,[d] Filip Uhlik,[e] María Ángeles Herranz,[c] Nazario Martín*[,c,f] Shigeru Nagase*[,g] and Takeshi Akasaka*[,d,h,i,j]

[a] *Institute for Integrated Cell-Material Sciences (WPI-iCeMS), Kyoto University, Sakyo-ku, Kyoto 606-8501, Japan*

[b] *Department of Chemistry and Biochemistry, National Chung-Cheng University, Min-Hsiung, Chia-Yi 62199, Taiwan-ROC*

[c] *Departamento de Química Orgánica I, Facultad de Química, Universidad Complutense, E-28040 Madrid, Spain*

[d] *Life Science Center of Tsukuba Advanced Research Alliance, University of Tsukuba, Tsukuba, Ibaraki 305-8577, Japan*

[e] *Department of Physical and Macromolecular Chemistry, Faculty of Science, Charles University in Prague, Albertov 6, 12843 Praha 2, Czech Republic*

[f] *IMDEA–Nanoscience, Campus de Cantoblanco, Madrid E-28049, Spain*

[g] *Fukui Institute for Fundamental Chemistry, Kyoto University, Sakyo-ku, Kyoto 606-8103, Japan*

[h] *Foundation for Advancement of International Science, Tsukuba, Ibaraki 305-0821, Japan*

[i] *Department of Chemistry, Tokyo Gakugei University, Tokyo 184-8501, Japan*

[j] *State Key Laboratory of Materials Processing and Die & Mould Technology, School of Materials Science and Technology, Huazhong University of Science and Technology, Wuhan 430074, China*

AUTHOR EMAIL ADDRESS: nazmar@quim.ucm.es, nagase@ims.ac.jp, akasaka@tara.tsukuba.ac.jp,

**RECEIVED DATE (to be automatically inserted after your manuscript is accepted if required according to the journal that you are submitting your paper to)**

**ABSTRACT:**

Synthesizing unprecedented diamagnetic adducts of an endohedral metallofullerene was achieved by using 1,3-dipolar cycloaddition reaction of paramagnetic La@$C_s$-$C_{82}$ with a simultaneous hydrogen addition. The selective formation of two main products, La@$C_s$-$C_{82}$HCMe$_2$NMeCHPh (**2a** and **2b**), was firstly detected by HPLC analysis and MALDI-TOF mass spectrometry. **2a** and **2b**-O, which was readily formed by the oxidation of **2b**, were isolated by multi-step HPLC separation and were fully-characterized by spectroscopic methods, including 1D and 2D-NMR, UV-vis-NIR measurements and electrochemistry. The hydrogen atom was found to be connected to the fullerene cage directly in the case of **2a**, and the redox behavior indicated that the C-H bond can still be readily oxidized. The reaction mechanism and the molecular structures of **2a** and **2b** were reasonably proposed by the interplay between experimental observations and DFT calculations. The feasible order of the reaction

process would involve a 1,3-dipolar cycloaddition followed by the hydrogen addition through a radical pathway. It is concluded that the characteristic electronic properties and molecular structure of La@$C_s$-$C_{82}$ resulted in a site-selective reaction, which afforded a unique chemical derivative of an endohedral metallofullerene in high yields. Derivative **2a** constitutes the first endohedral metallofullerene where the direct linking of a hydrogen atom has been structurally proven.

**INTRODUCTION:**

Endohedral metallofullerenes (EMFs)[1] – fullerenes which encapsulate metal atoms or clusters into their inner cavity – are novel materials which have attracted broad interests in a variety of research fields, such as chemistry, physics and biomaterial science.[1-4] Remarkable features of EMFs are unique molecular structures, and magnetic and electronic properties induced by the inside metals.[5] A number of reports are recently available for demonstrating the potential uses of EMFs as promising novel materials. Some relevant examples are the preparation of organic solar cells based on $Lu_3N@C_{80}$ derivatives which demonstrated higher open circuit voltage and power conversion efficiency than $PC_{61}BM$[3a] and, the highly efficient MRI contrast agent based on $Gd_3N@C_{80}$,[4a] just to name a few.[3,6,7]

For an easier accessibility to EMFs based materials, a wider availability of chemical functionalization methods on EMFs is required.[1d,8] Unique properties of EMFs may lead to unique chemical reactivities, such as selective radical addition[2c-e] and enantioselective cycloaddition.[2f] In this regard, despite the former efforts, much work is still needed for a better control on the chemical reactivity of the increasing variety of EMFs.

Among EMFs, paramagnetic EMFs are of particular interest because interplay between π-electron spins on the fullerene cage and inside metal atoms is expected to produce unconventional magnetic features. Its potential for spintronics devices has been demonstrated by several reports, which involve electrochemical switching of the magnetic properties,[9b] the high electron mobility (μ) exceeding 10 $cm^2$ $V^{-1}$ $s^{-1}$ of single-crystals of a derivative of La@$C_{2v}$-$C_{82}$,[3b] and so on.[10] However, radical reactivity that is

originated from the paramagnetic property of the EMFs often leads unprecedented chemical reactivities, such as the formation of singly-bonded derivative of La@$C_{2v}$-$C_{82}$ from the Bingel-Hirsch reaction[2a] or the selective radical coupling reactions,[2d,2e] of the fullerenes. For creating practical electronic and magnetic materials based on EMFs, a sophisticated management of chemical functionalization is essential on the basis of deep understanding of the unique properties of paramagnetic EMFs.

La@$C_{2v}$-$C_{82}$ is one of the most investigated EMFs and is considered as a prototype of paramagnetic EMFs, since it was demonstrated that a family of lanthanum-containing fullerenes could be produced and that extraction with toluene yielded mostly La@$C_{82}$.[11] La@$C_s$-$C_{82}$[12] which has been used for the present study is an isomer of La@$C_{2v}$-$C_{82}$. In contrast to the $C_{2v}$ isomer, however, a much lower number of reports are available for the chemical derivatization of La@$C_s$-$C_{82}$.[13] One reason of it is that La@$C_s$-$C_{82}$ has demonstrated relatively poor selectivity in addition reactions, resulting low yields in previous reports because of the lower symmetry relative to La@$C_{2v}$-$C_{82}$ and the presence of 44 nonequivalent carbon atoms.

We herein report an unprecedented chemical reactivity of a paramagnetic endohedral metallofullerene La@$C_s$-$C_{82}$. Surprisingly, we found that the 1,3-dipolar cycloaddition reaction of the fullerene, which is referred to as the Prato reaction,[14] affords two new adducts of La@$C_s$-$C_{82}$ in a highly selective way with an unprecedented and intriguing hydrogen addition reaction.

## RESULTS AND DISCUSSION:

### Synthesis and isolation of the two adducts

Firstly, the 1,3-dipolar cycloaddition reaction of La@$C_s$-$C_{82}$ (denoted as La@$C_{82}$ hereafter for simplicity) using an azomethine ylide as 1,3-dipole was conducted based on a standard procedure by using *o*-dichlorobenzene (*o*-DCB) as solvent (Scheme 1). After refluxing the reaction solution for 15 min, the HPLC profiles of the resulting solution showed different peaks with consumption of the starting La@$C_{82}$ (Figure 1a). The appearance of several shoulder peaks indicated that the selectivity of the addition reaction to the fullerene was quite low under these conditions.

Secondly, a droplet of toluene was added into the reaction solution of *o*-DCB before refluxing, and the selectivity of the addition reaction was drastically improved as confirmed by the HPLC profiles (Figure 1b). After refluxing for one hour, the HPLC profile of the reaction mixture indicated that approximate 50 % of the starting fullerene was consumed and two products were dominantly formed. This high selectivity in the reaction is notable since several adducts could be expected to form because of the 44 unequivalent carbon atoms of the La@$C_{82}$ cage.[12, 13a]

The two products were successfully isolated from the unreacted starting materials and byproducts by using multi-step high performance liquid chromatography (HPLC) (See the Supporting Information and Figure 2). The conversion yields of the main product (**2a**) and the minor product (**2b**) are 45 % and 20 %, respectively, based on the consumed La@$C_{82}$. These values are close to twofold in comparison with the best yield (24%) ever reported for the chemical functionalization of La@$C_{82}$.[13b]

**Characterization of the main product (2a)**

Matrix Assisted Laser Desorption Ionization, which is coupled to a Time-of-Flight analyzer (MALDI-TOF) mass spectrum, of **2a** shows a molecular ion peak at 1285 *m/z* and a fragment peak at 1123 *m/z* which came from pristine La@$C_{82}$ formed by the loss of the addend during laser desorption (Figure 3). It is notable that the molecular ion peak is not the expected 1284 *m/z* for the Prato adduct of La@$C_{82}$, and peaks between 1284 to 1289 *m/z* are not consistent with the isotopic distribution pattern of the usual Prato adduct. This result suggests that **2a** is a 1,3-dipolar cycloadduct which is accompanied by an additional hydrogen atom, and the small peak at 1284 *m/z* would be originated from the loss of the hydrogen atom of **2a**.

Generally, it is well known that the Prato adducts of La@$C_{2v}$-$C_{82}$ have open shell electronic structures as well as pristine La@$C_{2v}$-$C_{82}$.[11] In sharp contrast with the Prato adducts of La@$C_{2v}$-$C_{82}$ which have ever been reported, as indicated by the mass spectra, **2a** has a closed shell structure because of the addition of the hydrogen atom and accordingly, the electron spin resonance (ESR) spectra of **2a** showed no signal (data not shown). For further characterization, therefore, NMR measurements were conducted for **2a** as obtained. The $^{1}$H and $^{13}$C NMR spectra, respectively, demonstrated characteristic signals of the pyrrolidine ring, phenyl group and the hydrogen atom (Figures 4a and 5a). Their assignments were confirmed by DEPT 135 and 2D-

NMR measurements involving HSQC and HMBC (Figures S2-S4). The 2D-NMR spectra also provided reliable information on the addition position of the unexpected hydrogen atom. The $^{1}$H-NMR signal of the hydrogen atom at 3.19 ppm shows the clear correlation with carbon atoms of the fullerene cage both in HSQC and HMBC. These results indicate the direct connection between the hydrogen atom and the fullerene cage. It is also worth mentioning that the hydrogen atom is notably up-field shifted compared to dihydro, hydroalkylated and hydroarylated derivatives of $C_{60}$ (Table 1),[15] or the hydrogen atoms directly connected to $C_{60}$ cages after intramolecular nucleophilic additions of alcohols to $C_{60}$,[16] which suggests that the electron-withdrawing effect from La@$C_{82}$ is much weaker than that of $C_{60}$ and the hydrogen atom on La@$C_{82}$ is electron-rich. Furthermore, considering the chemical shift in the $^{1}$H NMR, could be stated that the hydrogen atom of **2a** shows a much lower acidity than those $C_{60}$ derivatives listed in Table 1. Indeed, the C-H bond on La@$C_{82}$ can be readily oxidized (*vide infra*) as well as in the case of La@$C_{2v}$-$C_{82}$.[17]

**Characterization of the minor product (2b)**

Just after the isolation by HPLC, **2b** mainly showed a molecular ion peak at 1285 *m/z* and a fragment peak at 1123 *m/z* in MALDI-TOF mass measurement as well as **2a** (Figure 6a). However, after a few minutes from the isolation under ambient conditions, the minor product showed a different spectral pattern which is attributed to an oxidized **2b** (**2b**-O) at 1301 *m/z* (Figure 6b) instead of **2b**. This oxidation process was also confirmed by HPLC analysis in which the elution time of **2b** (12.8 min) was extended as the oxidation on **2b** progressed to afford **2b**-O (13.2 min) (Figure 2). In contrast to **2b**, **2a** is much more stable and its spectra were almost unchanged after three days stored under ambient conditions without light. Although the reasons for the significant different stabilities of **2a** and **2b** are still not completely clear, it may be explained by the fact that the stability and electronic structures of the compounds can be influenced by the different direction of the addend, in particular the phenyl ring, in **2a** and **2b**, as indicated by DFT calculation (*vide infra*).

Although the instability of **2b** made it hard to accomplish further characterization, investigation on **2b**-O provided the sufficient structural information which is associated with **2b**. **2b**-O has also a closed shell

structure as well as **2a** and, therefore, NMR measurements were performed. The $^{1}$H and $^{13}$C-NMR spectra are distinguishable from those of **2a**, and all characteristic peaks of the addend and the hydrogen atom were discernible (Figure 4b and 5b). Meanwhile, HSQC spectra revealed striking difference between **2a** and **2b**-O (Figure S5). In the HSQC spectra of **2b**-O, no correlation was observed between the hydrogen atom and the carbon atoms of the $C_{82}$ cage. This result suggested that the oxidized position is the bond between the hydrogen atom and the adjacent carbon atom of the cage, and a hydroxyl moiety was formed as the result of the oxidation. This fact was confirmed by the $^{1}$H-NMR measurement of **2b**-O following mixing of the sample solution of **2b**-O with $D_2O$ (Figure S6). The disappearance of the proton signal of the hydrogen atom unambiguously indicates that the hydrogen atom belongs to a hydroxyl group and formation of an epoxide is excluded as the result of the oxidation (Scheme 2).

**Discussion on the reaction mechanism and molecular structures of 2a and 2b-O**

In the present reaction, the hydrogen addition was a key for affording **2a** and **2b**-O in relatively high yields. Because the reaction without addition of toluene before heating afforded a vast number of adducts as demonstrated in Figure 1a, some Prato adducts were possibly formed and they resulted to be somehow unstable and evolved to a variety of different compounds. It is also indicated by the shorter reaction time (<15 min.) in the case of the absence of toluene to consume the half amount of starting La@$C_{82}$ than the reaction using a droplet of toluene (~60 min.). Therefore, a plausible explanation for affording several products in the former reaction would be overreaction and multiple addition of the addends to the fullerene. MALDI-TOF mass spectrum of the reaction mixture indicated the existence of different compounds such as pristine La@$C_{82}$, the Prato mono-adduct (La@$C_{82}CMe_2NMeCHPh$), bis-adducts and their respective oxidized compounds (Figure S7).

Arguments can be made for (i) the origin of the hydrogen atom and, (ii) the prior reaction between the additions of the hydrogen and azomethine ylide (Path A and B in Scheme 3).

Two possibilities were considered for the origin of the hydrogen atom: generation of water molecules steaming from the formation of azomethine ylide or, alternatively, a hydrogen atom from toluene. To get rid

of the first possibility, we carried out the 1,3-dipolar cycloaddition reaction in *o*-DCB solution containing $D_2O$ and a droplet of toluene. The MALDI-TOF mass spectra of the resulting adducts (not shown) did not show any evidence for the addition of the deuterium atom and only showed a molecular ion peak at 1285 *m/z* which indicates the existence of a product with the hydrogen atom. These experimental findings reveal that the origin of the hydrogen is not the water molecule which was generated in the formation of azomethine ylide. Therefore, toluene appears as the most probable origin for the hydrogen atom.

In order to confirm the above finding, the reactivity of La@$C_{82}$ towards toluene was examined by heating La@$C_{82}$ with a droplet of toluene in carefully degassed *o*-DCB. It is notable that a large portion of La@$C_{82}$ was unchanged after refluxing for one hour (Figure S8). This result indicates that the reaction proceeds much slower than that of the 1,3-cycloaddition reaction. MALDI-TOF mass spectrum of the reaction mixture showed a new peak at 1156 *m/z*, which is attributed to La@$C_{82}HO_2$, with a small fragment peak at 1155 *m/z* which stems from the loss of the hydrogen atom (Figure S9). The formation of La@$C_{82}HO_2$ implies that La@$C_{82}$H was formed under these reaction conditions and readily oxidized during the process of preparing samples for MALDI-TOF mass measurements under ambient atmosphere. A similar rapid oxidation has also been reported for another isomer of La@$C_{82}$ (La@$C_{2v}$-$C_{82}$).[15] As mentioned above, because the addition of hydrogen atom is much slower than the Prato reaction in the absence of toluene, it is reasonable to conclude that the prior addition of azomethine ylide (Path A) is the dominating reaction pathway and the formation of La@$C_{82}CMe_2NMeCHPh$ (**1**) can occur prior to the hydrogen addition.

The molecular structures of **2a** and **2b** were confirmed by the interplay between experimental results and theoretical calculations. Absorption spectra of **2a** and **2b**-O demonstrate their strong resemblance (Figure 7). Generally, absorption spectra in visible-NIR region of the fullerene derivatives provide sufficiently distinctive fingerprints of the π-electron system topology.[1] In short, the spectra directly reflect the addition position of the addend on the fullerene cage. Hence, the remarkable similarity between **2a** and **2b**-O indicates that the two compounds are the same site-isomers ("site-isomer" is a classification in fullerenes proposed recently by Martín et al.[18]) having the same addition sites of the pyrrolidine ring and the hydrogen atom, despite the presence of 44 possible addition positions in the starting La@$C_{82}$.

DFT calculations[19-22] give us sufficient criteria for the prediction of the addition sites of the substituents. Regarding the 1,3-dipolar cycloaddition of an azomethine ylide to fullerenes, on the one hand, the LUMO of the dipolarophile plays an important role.[23] In addition, a pair of the carbon atoms which have relatively high positive charge and high POAV[24] value simultaneously, and the adjacent carbon atom with a relatively negative charge, should be the most feasible candidate site for the cycloaddition of diamagnetic endohedral metallofullerenes.[2f,25] La@$C_{82}$ has the one site where these criteria are fulfilled, that is C20-C21 (Figure 8, Table 2 and Supporting Information). Furthermore, it has previously been reported that the intrinsic radical character of azomethine ylides[26] may play an important role in 1,3-dipolar cycloadditions on paramagnetic endohedral metallofullerenes.[9b,27] In this case, the feasible addition site contains the carbon atom which has the largest POAV and spin density, in addition to an adjacent carbon atom with a relatively large negative charge. Therefore, C22-C23 is the best candidate fulfilling these criteria (Figure 8, Tables 2, 4 and Supporting Information).

On the basis of the first criterion, the bond between C20-C21 potentially affords four regioisomers, each one having two conformers of **1** as depicted in Figure 9 and S11. The relative formation energies were calculated for the possible eight optimized structures. It is found in all cases that the more stable structure has the methyl group connected to the nitrogen atom, located far away from the phenyl group. Among the most stable four structures, *A1* and *B1* demonstrate better stabilities and may be considered as the intermediates for **2b** and **2a**, respectively, based on the relative formation energies. However, a remarkable difference was not found in the charge density, spin density or POAV values among these possible intermediates and the starting La@$C_{82}$ (Table 3 and the Supporting information). Therefore, the subsequent selective addition of H atom cannot be rationalized by this first criterion.

The second criterion considering the radical reactivity suggests the feasibility of C22-C23 as the addition site. Moreover, it is supported by the ROESY measurements on **2a** which demonstrate a correlation between the hydrogen atom in the pyrrolidine ring and the hydrogen atom on the fullerene cage (Figure S12). This result indicates the fact that the pyrrolidine moiety and the hydrogen atom of **2a** must locate within a distance for nuclear Overhauser effect, that is usually within 5 Å, being consistent in the addition position of

C22-C23. Judging from the optimized structures by the DFT calculations (Figure 10 and S13), firstly, the stable conformation of the pyrrolidine ring is the same to those in the adducts based on C20-C21. The relative energies suggest that the most feasible structures are *Structures A'1* and *B'1*. Although these energies are higher than those based on C20-C21, it is safe to conclude that the relative energies are not significant enough for the determination of the structure because the second criterion is based on the radical reactivity, in which kinetic products are favorable rather than the thermodynamic products. In addition, in sharp contrast to *Structures A1* and *B1*, *Structures A'1* and *B'1* explain the selectivity of the following hydrogen addition. Regarding the addition position of the hydrogen atom, the carbon atom C3 is the best candidate because it has the highest spin density and POAV values both in pristine La@$C_{82}$ and the intermediates **1** (Table 3). Moreover, the spin density is remarkably increased in **1** (0.12-0.14) relative to pristine fullerene (0.09), rationalizing the site-selective addition of the hydrogen atom. It has previously been reported that radical addition on La@$C_{82}$ occurs on the carbon atom having the highest spin density and POAV values.[2d] All taken together, the molecular structures of **2a** and **2b** are concluded to be *Structures A'1*+$H_{C3}$ and B'1+$H_{C3}$, respectively, as it is shown in Figure 11.

This result is in good agreement with the experimental findings where the two adducts were obtained in a selective way as a result of the addition reaction by an asymmetric azomethine ylide and in different yields.

**Optoelectronic properties of 2a and 2b-O**

UV-vis-NIR absorption spectra of **2a** and **2b**-O revealed changes in the electronic properties of the fullerene cage from pristine La@$C_{82}$ (Figure 7). In both compounds, the absorbance onsets show remarkable hypsochromic shifts from *ca.* 2000 nm in pristine La@$C_{82}$ to 1070 nm, which is attributed to the loss of open-shell electronic structure and the formation of closed-shell structures.

Electrochemical measurements of **2a** and **2b**-O were performed by cyclic voltammetry (CV) and differential pulse voltammetry (DPV) (Figure 12). The redox potentials were determined by DPV (Table 5). The first reduction and the first and second oxidation potentials are comparable between **2a** and **2b**-O. These

experimental findings are consistent with the absorption spectra, which demonstrate the similar electronic properties in both compounds. Meanwhile, **2a** and **2b**-O revealed distinguishable electrochemical stability in *o*-DCB. **2a** showed two small peaks at -0.35 and -0.80 V vs. $Fc/Fc^+$ couple when a freshly prepared sample was measured. Two peaks were found to become larger after scanning a more positive region than the first oxidation peak (0.27 V), which was confirmed by multiple scan in CV (Figure S14). **2b**-O demonstrated a similar behavior after the scan of the first oxidation peak. In addition, a new peak, which was not clearly detected in DPV but in CV measurements, appeared in the anodic region close to the oxidation peak during the scanning. These results suggest that the first oxidation step is attributable to the oxidation on the hydrogen atom, which leads to an irreversible reaction of decomposition of **2a** and **2b**-O and afforded new products which possess similar reduction potentials to those of paramagnetic pristine $La@C_{82}$. Moreover, it was revealed that the carbon bearing the hydrogen atom of **2a** and **2b**-O is still reactive towards oxidation reactions.

## CONCLUSIONS

Starting from Prato cycloadducts, we have found an unprecedented and intriguing chemical derivatization method affording less-explored functionalized $La@C_s$-$C_{82}$ in the highest conversion yields and site-selectivity among those reported chemical modifications for this endofullerene to date. Resulting adducts **2a** and **2b** are diamagnetic and the structures have been fully characterized by the interplay between experimental results and theoretical calculations. **2a** is the first example of a structurally characterized endohedral metallofullerene derivative which is directly linked with a hydrogen atom. **2b** was found to be relatively unstable and readily oxidized to **2b**-O in a few minutes under ambient conditions. Furthermore, **2a** and **2b**-O showed irreversible oxidation steps stemming from the oxidation of the hydrogen atom at relatively low potentials (~0.2 V vs. $Fc/Fc^+$ couple). Considering the availability of starting endohedral fulleropyrrolidines, this unprecedented behavior in fullerene chemistry may inspire further chemical modifications by utilizing the reactive C-H bond as a

foothold for further C-H activation reactions,[28] thus opening a new avenue in the chemical reactivity of modified metallofullerenes.

## EXPERIMENTAL SECTION:

**General.** All chemicals and solvents were obtained from Wako Inc. and used without further purification unless otherwise stated. La@$C_s$-$C_{82}$ was prepared according to the reported procedure.[17] Partially deuterated 2-(methylamino)isobutyric acid ($MeNDCMe_2COOD$) was synthesized by heating the acid in $D_2O$ overnight and dried under reduced pressure. *o*-DCB was distilled over calcium hydride in a reduced pressure under an argon atmosphere and toluene was distilled over benzophenone sodium ketyl under an argon atmosphere prior to use in reactions. Analytical and preparative high performance liquid chromatography (HPLC) were performed on a JASCO HPLC apparatus or JAI LC-908. Toluene was used as the eluent. The $^1H$, $^{13}C$ and 2D NMR measurements were carried out on a Bruker AVANCE 500 spectrometer with a CryoProbe system, where TMS was used as an internal reference ($\delta$ = 0.00 ppm). Absorption spectra were recorded in a SHIMADZU UV-3150 spectrophotometer. Mass spectrometry was performed on a Bruker BIFLEX III, using 1,1,4,4-tetraphenyl-1,3-butadiene as a matrix. The samples were prepared by drop casting in ambient conditions. Cyclic voltammograms (CVs) and differential pulse voltammograms (DPVs) were recorded on a BAS CV50W electrochemical analyzer. Platinum wires were used as the working and counter electrodes. The reference electrode was a saturated calomel reference electrode (SCE) filled with 0.1 M ($n$-Bu)$_4NPF_6$ ($TBAPF_6$) in *o*-DCB. CVs were recorded using a scan rate of 50 mV/s, and DPVs were obtained using a pulse amplitude of 50 mV, a pulse width of 50 ms a pulse period of 200 ms, and a scan rate of 20 mV/s. The solution was deaerated for 20 min. with argon prior to the electrochemical measurements.

**Prato reaction of La@$C_{82}$ in *o*-ODCB.** 1.0 mL *o*-DCB solution containing 0.25 mg of La@$C_s$-$C_{82}$ ($2.3 \times 10^{-4}$ mmol) was carefully degassed and refluxed with 6 equivalents of 2-(methylamino)isobutyric

acid and 2 equivalents of benzaldehyde under argon atmosphere. After cooling to the room temperature, the reaction mixture was analyzed by HPLC (Figure 1a).

**Synthesis of pyrrolidine adducts 2a and 2b.** 25 mL *o*-DCB solution containing 6.4 mg of La@$C_s$-$C_{82}$ ($5.7 \times 10^{-3}$ mmol) and 50 μL of toluene was carefully degassed and refluxed with 6.0 equivalents of 2-(methylamino)isobutyric acid and 2.0 equivalents of benzaldehyde under argon atmosphere. After cooling to the room temperature, the solvent was removed under reduced pressure and reaction mixture was subjected to multi step preparative HPLC system as shown in Figure S1 for the isolation of the target compound from byproducts and unreacted starting materials. As the result, **2a** was obtained in 45% yield based on the consumed starting fullerene, which was confirmed by the HPLC analyses. **2b** was also obtained after the HPLC separation and was found to become oxidized (**2b**-O) in a few minutes. The conversion yield of **2b**-O was 20% based on the recovered fullerene.

*La@$C_{82}$CHMe$_2$NMeCHPh (**2a**)*: $^1$H NMR (500 MHz, $CS_2$/$CD_2Cl_2$ = 3/1 (v/v)) δ 7.56 (d, *J* = 7.3 Hz, 1H), 7.46 (m, 2H), 7.33 (m, 1H), 7.13 (t, *J* = 7.2 Hz, 1H), 4.43 (s, 1H, C*H*), 3.19 (s, 1H, C*H* on the cage), 2.39 (s, 3H, NC*H*$_3$), 1.61 (s, 3H, CC*H*$_3$), 1.54 (s, 3H, CC*H*$_3$); $^{13}$C NMR (125 MHz, $CS_2$/$CD_2Cl_2$ = 3/1 (v/v)) δ 163.24, 156.13, 155.59, 152.80, 151.66, 150.63, 150.35, 150.22, 150.08, 149.94, 149.62, 149.25, 148.76, 148.15, 147.99, 147.63, 146.62, 146.60, 146.45, 146.24, 146.16, 146.10, 145.85, 145.81, 145.42, 145.13, 144.54, 144.17, 143.63, 143.32, 142.98, 142.95, 142.67, 142.52, 142.36, 142.31, 141.81, 141.74, 141.33, 141.10, 139.89, 139.65, 139.50, 139.13, 138.33, 138.05, 138.00, 137.92, 137.73, 137.71, 137.63, 137.59, 137.45, 136.80, 136.18, 136.07, 135.80, 135.74, 135.63, 135.54, 135.16, 134.93, 134.17, 133.32, 133.17, 133.11, 132.90, 132.70, 132.26, 131.26, 131.20, 130.59, 130.50, 129.55, 129.47, 129.35, 129.28, 129.15, 129.02, 128.96, 128.73, 128.34, 127.94, 127.20, 127.02, 77.91 (*C*H), 68.23 (*C*(CH$_3$)$_2$), 64.76, 62.57, 47.62 (*C*H on the cage), 32.13(NC*H*$_3$), 26.78 (*C*H$_3$), 16.26 (*C*H$_3$); DEPT135 (125 MHz, $CS_2$ with acetone-$d_6$ in a capillary tube) δ 131.17 (*C*H), 130.50 (*C*H), 129.28 (*C*H), 128.72 (*C*H), 128.34 (*C*H),

77.91 (*C*H), 47.62 (*C*H on the cage), 32.13 (N*C*H$_3$), 26.78 (*C*H$_3$), 16.26 (*C*H$_3$); UV-vis-NIR (in $CS_2$) $\lambda_{max}$ 520, 944; MALDI-TOF mass calculated for $C_{93}H_{16}LaN$ ([*M*]$^-$): 1285.0, found: 1285.2 *m/z*.

*La@C$_{82}$COHMe$_2$NMeCHPh (**2b**-O)*: $^1$H NMR (500 MHz, $CS_2/CD_2Cl_2$ = 3/1 (v/v)) δ 7.54 (m, 1H), 7.42 (m, 1H), 7.33 (m, 1H), 7.14 (m, 1H), 6.90 (m, 1H), 4.36 (s, 1H, C*H*), 3.53 (s, 1H, CO*H*), 2.26 (s, 3H, NC*H$_3$*), 1.84 (s, 3H, CC*H$_3$*), 1.60 (s, 3H, CC*H$_3$*); $^{13}$C NMR (125 MHz, $CS_2$ with acetone-*d*$_6$ in a capillary tube) δ 159.82, 158.59, 156.12, 155.78, 153.78, 152.71, 151.68, 150.85, 150.43, 150.35, 149.96, 149.89, 149.24, 149.12, 148.86, 148.70, 148.59, 147.81, 147.11, 146.94, 146.45, 146.28, 145.96, 145.79, 145.74, 145.58, 145.02, 144.66, 144.22, 143.53, 143.39, 143.24, 143.01, 142.82, 142.72, 142.06, 141.86, 141.62, 141.02, 140.92, 140.87, 140.33, 140.00, 139.51, 139.44, 139.07, 138.93, 138.60, 137.88, 137.84, 137.69, 137.55, 137.47, 137.35, 137.22, 137.19, 136.93, 136.65, 136.16, 135.61, 135.51, 135.35, 135.20, 135.06, 134.63, 134.59, 134.10, 133.25, 132.59, 132.25, 131.66, 131.32, 131.01, 130.82, 130.46, 130.36, 130.07, 129.42, 128.06, 127.89, 127.38, 127.14, 125.78, 77.77 (*C*H), 73.52 (*C*OH), 68.99, 68.97 (*C*(CH$_3$)$_2$), 59.40, 32.17 (N*C*H$_3$), 26.04 (*C*H$_3$), 17.08 (*C*H$_3$); UV-vis-NIR (in $CS_2$) $\lambda_{max}$ 525, 945; MALDI-TOF mass calculated for $C_{93}H_{16}OLaN$ ([*M*]$^-$): 1301.0, found: 1301.1 *m/z*.

**Thermal reaction of La@C$_{82}$ with a droplet of toluene in *o*-ODCB.** 1.0 mL *o*-DCB solution containing 0.25 mg of La@*C$_s$*-$C_{82}$ ($2.3 \times 10^{-4}$ mmol) and 5 μL of toluene was carefully degassed and refluxed under argon atmosphere. After cooling to the room temperature, the reaction mixture was analyzed by HPLC.

**Thermal reaction of La@C$_{82}$ with *o*-ODCB containing D$_2$O.** 1.0 mL *o*-DCB was stirred with 0.5 mL of $D_2O$ for 15 min, then the organic layer was corrected and used for the reaction as below. 1.0 mL of the *o*-DCB solution containing 0.25 mg of La@*C$_s$*-$C_{82}$ ($2.3 \times 10^{-4}$ mmol) and 5 μL of toluene was

carefully degassed and refluxed under argon atmosphere. After cooling to the room temperature, the reaction mixture was analyzed by HPLC and MALDI-TOF mass measurements.

**Theoretical calculations.** Geometries were optimized using the Gaussian 09 program[19] with the M06-2X[20] functional. The SDD basis set with relativistic effective core potential suggested by Cao and Dolg[21] was used for La atom. The split valence 3-21G[22a] or 6-31G*[22b,c] basis sets were used for H, C and N atoms.

**ACKNOWLEDGMENTS:**

The Strategic Japanese–Spanish Cooperative Program funded by JST and MINECO (PIB2010JP-00196). The iCeMS is supported by World Premier International Research Center Initiative (WPI), MEXT, Japan. FU is supported from grants of the Ministry of Education of the Czech Republic & the MetaCentrum computing facility (MSM0021620857 & LM2010005). The Ministerio de Economía y Competitividad (MINECO) of Spain (project CTQ2011-24652), the CAM (MADRISOLAR-2 project S2009/PPQ-1533), and the European Research Council via ERC-2012-ADG_20120216 (Chirallcarbon) is acknowledged. This work is also supported by Financial supports from research on Innovative Areas (20108001, "p-Space"), Grants-in-Aid for Scientific Research (A) (202455006), (B) (24350019), Young Scientists (B) (25810098), the Next Generation Super Computing Project (Nanoscience Project), the Nanotechnology Support Project, Grants-in-Aid for Scientific Research on Priority Area (20036008 and 20038007), a Specially Promoted Research Grant (22000009) from the Ministry of Education, Culture, Sports, Science, and Technology of Japan. N. M. is indebted to Alexander von Humboldt Foundation.

**Supporting Information Available:**

Spectral data of the compounds, Cartesian coordinates of the optimized structures. This material is available free of charge via the Internet at http://pubs.acs.org.

**REFERENCES:**


(1) For reviews, see: (a) *Chemistry of Nanocarbons*, Akasaka, T., Wudl, F., Nagase, S., Eds., Wiley, Chichester, 2010. (b) Chaur, M. N.; Melin, F.; Ortiz, A. L.; Echegoyen, L. *Angew. Chem. Int. Ed.* **2009**, *48*, 7514. (c) Rudolf, M.; Wolfrum, S.; Guldi, D. M.; Feng, L.; Tsuchiya, T.; Akasaka, T.; Echegoyen, L. *Chem. Eur. J.* **2012**, *18*, 5136. (d) Popov, A. A.; Yang, S.; Dunsch, L. *Chem. Rev.* **2013**, *113*, 5989. (e) Nagase, S. *Bull. Chem. Soc. Jpn.* **2014**, *87*, 167.

(2) (a) Feng, L.; Nakahodo, T.; Wakahara, T.; Tsuchiya, T.; Maeda, Y.; Akasaka, T.; Kato, T.; Horn, E.; Yoza, K.; Mizorogi, N.; Nagase, S. *J. Am. Chem. Soc.* **2005**, *127*, 17136. (b) Lu, X.; Nikawa, H.; Nakahodo, T.; Tsuchiya, T.; Ishitsuka, M. O.; Maeda, Y.; Akasaka, T.; Toki, M.; Sawa, H.; Slanina, Z.; Mizorogi, N.; Nagase, S. *J. Am. Chem. Soc.* **2008**, *130*, 9129. (c) Shu, C. Y.; Slebodnick, C.; Xu, L. S.; Champion, H.; Fuhrer, T.; Cai, T.; Reid, J. E.; Fu, W. J.; Harich, K.; Dorn, H. C.; Gibson, H. W. *J. Am. Chem. Soc.* **2008**, *130*, 17755. (d) Takano, Y.; Yomogida, A.; Nikawa, H.; Yamada, M.; Wakahara, T.; Tsuchiya, T.; Ishitsuka, M. O.; Maeda, Y.; Akasaka, T.; Kato, T.; Slanina, Z.; Mizorogi, N.; Nagase, S. *J. Am. Chem. Soc.* **2008**, *130*, 16224. (e) Takano, Y.; Ishitsuka, M. O.; Tsuchiya, T.; Akasaka, T.; Kato, T.; Nagase, S. *Chem. Commun.* **2010**, *46*, 8035. (f) Sawai, K.; Takano, Y.; Izquierdo, M.; Filippone, S.; Martin, N.; Slanina, Z.; Mizorogi, N.; Waelchli, M.; Tsuchiya, T.; Akasaka, T.; Nagase, S. *J. Am. Chem. Soc.* **2011**, *133*, 17746.

(3) (a) Ross, R. B.; Cardona, C. M.; Guldi, D. M.; Sankaranarayanan, S. G.; Reese, M. O.; Kopidakis, N.; Peet, J.; Walker, B.; Bazan, G. C.; Van Keuren, E.; Holloway, B. C.; Drees, M. *Nat. Mater.* **2009**, *8*, 208. (b) Sato, S.; Seki, S.; Honsho, Y.; Wang, L.; Nikawa, H.; Luo, G.-F.; Lu, J.; Haranaka, M.; Tsuchiya, T.; Nagase, S.; Akasaka, T. *J. Am. Chem. Soc.* **2011**, *133*, 2766.

(4) (a) Zhang, J. F.; Fatouros, P. P.; Shu, C. Y.; Reid, J.; Owens, L. S.; Cai, T.; Gibson, H. W.; Long, G. L.; Corwin, F. D.; Chen, Z. J.; Dorn, H. C. *Bioconjugate Chem.* **2010**, *21*, 610. (b) Wilson, J.

D.; Broaddus, W. C.; Dorn, H. C.; Fatouros, P. P.; Chalfant, C. E.; Shultz, M. D. *Bioconjugate Chem.* **2012**, *23*, 1873. (c) Yang, K. N.; Cao, W. P.; Hao, X. H.; Xue, X.; Zhao, J.; Liu, J.; Zhao, Y. L.; Meng, J.; Sun, B. Y.; Zhang, J. C.; Liang, X. J. *Nanoscale* **2013**, *5*, 1205.

(5) (a) Rodriguez-Fortea, A.; Balch, A. L.; Poblet, J. M. *Chem. Soc. Rev.* **2011**, *40*, 3551. (b) Xing, L.; Akasaka, T.; Nagase, S. *Chem. Commun.* **2011**, *47*, 5942.

(6) Tsuchiya, T.; Kumashiro, R.; Tanigaki, K.; Matsunaga, Y.; Ishitsuka, M. O.; Wakahara, T.; Maeda, Y.; Takano, Y.; Aoyagi, M.; Akasaka, T.; Liu, M. T.; Kato, T.; Suenaga, K.; Jeong, J. S.; Iijima, S.; Kimura, F.; Kimura, T.; Nagase, S. *J. Am. Chem. Soc.* **2008**, *130*, 450.

(7) Wang, Z. N.; Li, X. F.; Yang, S. H. *Langmuir* **2009**, *25*, 12968.

(8) (a) *Fullerenes*, Hirsch, A., Brettreich, M., Eds., Wiley-VCH, Weinheim, 2004. (b) *Carbon Nanotubes and Related Structures*, Guldi, D. M., Martín, N. Eds., Wiley-VCH, Weinheim, 2010.

(9) (a) Yasutake, Y.; Shi, Z. J.; Okazaki, T.; Shinohara, H.; Majima, Y. *Nano Lett.* **2005**, *5*, 1057. (b) Crivillers, N.; Takano, Y.; Matsumoto, Y.; Casado-Montenegro, J.; Mas-Torrent, M.; Rovira, C.; Akasaka, T.; Veciana, J. *Chem. Commun.* **2013**, *49*, 8145.

(10) (a) Okimoto, H.; Kitaura, R.; Nakamura, T.; Ito, Y.; Kitamura, Y.; Akachi, T.; Ogawa, D.; Imazu, N.; Kato, Y.; Asada, Y.; Sugai, T.; Osawa, H.; Matsushita, T.; Muro, T.; Shinohara, H. *J. Phys. Chem. C* **2008**, *112*, 6103. (b) Takano, Y.; Aoyagi, M.; Yamada, M.; Nikawa, H.; Slanina, Z.; Mizorogi, N.; Ishitsuka, M. O.; Tsuchiya, T.; Maeda, Y.; Akasaka, T.; Kato, T.; Nagase, S. *J. Am. Chem. Soc.* **2009**, *131*, 9340. (c) Iwamoto, M.; Ogawa, D.; Yasutake, Y.; Azuma, Y.; Umemoto, H.; Ohashi, K.; Izumi, N.; Shinohara, H.; Majima, Y. *J. Phys. Chem. C* **2010**, *114*, 14704. (d) Zhao, S. X.; Zhang, J.; Dong, J. Q.; Yuan, B. K.; Qiu, X. H.; Yang, S. Y.; Hao, J. A.; Zhang, H.; Yuan, H.; Xing, G. M.; Zhao, Y. L.; Sun, B. Y. *J. Phys. Chem. C* **2011**, *115*, 6265.

(e) Kaneko, S.; Wang, L.; Luo, G. F.; Lu, J.; Nagase, S.; Sato, S.; Yamada, M.; Slanina, Z.; Akasaka, T.; Kiguchi, M. *Phys. Rev. B* **2012**, *86*.

(11) Chai, Y.; Guo, T.; Jin, C. M.; Haufler, R. E.; Chibante, L. P. F.; Fure, J.; Wang, L. H.; Alford, J. M.; Smalley, R. E. *J. Phys. Chem.* **1991**, *95*, 7564.

(12) Akasaka, T.; Wakahara, T.; Nagase, S.; Kobayashi, K.; Waelchli, M.; Yamamoto, K.; Kondo, M.; Shirakura, S.; Maeda, Y.; Kato, T.; Kako, M.; Nakadaira, Y.; Gao, X.; Van Caemelbecke, E.; Kadish, K. M. *J. Phys. Chem. B* **2001**, *105*, 2971.

(13) (a) Tagmatarchis, N.; Taninaka, A.; Shinohara, H. *Chem. Phys. Lett.* **2002**, *355*, 226. (b) Akasaka, T.; Kono, T.; Matsunaga, Y.; Wakahara, T.; Nakahodo, T.; Ishitsuka, M. O.; Maeda, Y.; Tsuchiya, T.; Kato, T.; Liu, M. T. H.; Mizorogi, N.; Slanina, Z.; Nagase, S. *J. Phys. Chem. A* **2008**, *112*, 1294.

(14) (a) Maggini, M.; Scorrano, G.; Prato, M. *J. Am. Chem. Soc.* **1993**, *115*, 9798; (b) Prato, M.; Maggini, M. *Acc. Chem. Res*. **1998**, *31*, 519.

(15) (a) Henderson, C. C.; Cahill, P. A. *Science* **1993**, *259*, 1885. (b) Keshavarz, M.; Knight, B.; Srdanov, G.; Wudl, F. *J. Am. Chem. Soc.* **1995**, *117*, 11371. (c) Jousselme, B.; Sonmez, G.; Wudl, F. *J. Mater. Chem.* **2006**, *16*, 3478. (d) Matsuo, Y.; Zhang, Y.; Nakamura, E. *Org. Lett.* **2008**, *10*, 1251. (e) Tzirakis, M. D.; Alberti, M. N.; Nye, L. C.; Drewello, T.; Orfanopoulos, M. *J Org. Chem.* **2009**, *74*, 5746. (f) Yang, W. W.; Li, Z. J.; Gao, X. A. *J Org. Chem.* **2010**, *75*, 4086. (g) Kuvychko, I. V.; Shustova, N. B.; Avdoshenko, S. M.; Popov, A. A.; Strauss, S. H.; Boltalina, O. V. *Chem. Eur. J.* **2011**, *17*, 8799.

(16) (a) Izquierdo, M.; Osuna, S.; Filippone, S.; Martín-Domenech, A.; Solà, M.; Martín, N. *J. Org. Chem.* **2009**, *74*, 1480. (b) Izquierdo, M.; Osuna, S.; Filippone, S.; Martín-Domenech, A.; Solà, M.; Martín, N. *J. Org. Chem.* **2009**, *74*, 6253.

(17) Akasaka, T.; Wakahara, T.; Nagase, S.; Kobayashi, K.; Waelchli, M.; Yamamoto, K.; Kondo, M.; Shirakura, S.; Okubo, S.; Maeda, Y.; Kato, T.; Kako, M.; Nakadaira, Y.; Nagahata, R.; Gao, X.; Van Caemelbecke, E.; Kadish, K. M. *J. Am. Chem. Soc.* **2000**, *122*, 9316.

(18) Maroto, E. E.; de Cozar, A.; Filippone, S.; Martin-Domenech, A.; Suarez, M.; Cossio, F. P.; Martín, N. *Angew. Chem., Int. Ed.* **2011**, *50*, 6060.

(19) Frisch, M. J.; Trucks, G. W.; Schlegel, H. B.; Scuseria, G. E.; Robb, M. A.; Cheeseman, J. R.; Scalmani, G.; Barone, V.; Mennucci, B.; Petersson, G. A.; Nakatsuji, H.; Caricato, M.; Li, X.; Hratchian, H. P.; Izmaylov, A. F.; Bloino, J.; Zheng, G.; Sonnenberg, J. L.; Hada, M.; Ehara, M.; Toyota, K.; Fukuda, R.; Hasegawa, J.; Ishida, M.; Nakajima, T.; Honda, Y.; Kitao, O.; Nakai, H.; Vreven, T.; Montgomery, Jr., J. A.; Peralta, J. E.; Ogliaro, F.; Bearpark, M.; Heyd, J. J.; Brothers, E.; Kudin, K. N.; Staroverov, V. N.; Kobayashi, R.; Normand, J.; Raghavachari, K.; Rendell, A.; Burant, J. C.; Iyengar, S. S.; Tomasi, J.; Cossi, M.; Rega, N.; Millam, J. M.; Klene, M.; Knox, J. E.; Cross, J. B.; Bakken, V.; Adamo, C.; Jaramillo, J.; Gomperts, R.; Stratmann, R. E.; Yazyev, O.; Austin, A. J.; Cammi, R.; Pomelli, C. J.; Ochterski, W.; Martin, R. L.; Morokuma, K.; Zakrzewski, V. G.; Voth, G. A.; Salvador, P.; Dannenberg, J. J.; Dapprich, S.; Daniels, A. D.; Farkas, O.; Foresman, J. B.; Ortiz, J. V.; Cioslowski, J. and Fox, D. J. GAUSSIAN 09, Revision A.02; Gaussian, Inc., Wallingford CT, 2009.

(20) Zhao, Y.; Truhlar, D.G. *Theor. Chem. Acc.* **2008**, *120*, 215.

(21) Cao, X. Y.; Dolg, M. *J. Mol. Struct. (Theochem)* **2002**, *581*, 139.

(22) (a) Binkley, J. S.; Pople J. A.; Hehre, W. J. *J. Am. Chem. Soc.* **1980**, *102*, 939. (b) Ditchfield, R.; Hehre, W. J.; Pople, J. A. *J. Chem. Phys.* **1971**, *54*, 724. (c) Hehre, W. J.; Ditchfield, R.; Pople, J. A. *J. Chem. Phys.* **1972**, *56*, 2257.

(23) (a) Sustmann, R. *Tetra. Lett.* **1971**, 2717. (b) Coldham, I.; Hufton, R. *Chem. Rev.* **2005**, *105*, 2765.

(24) Haddon, R. C. *Science* **1993**, *261*, 1545.

(25) (a) Takano, Y.; Obuchi, S.; Mizorogi, N.; Garcia, R.; Herranz, M. A.; Rudolf, M.; Wolfrum, S.; Guldi, D. M.; Martin, N.; Nagase, S.; Akasaka, T. *J. Am. Chem. Soc.* **2012**, *134*, 16103. (b) Aroua, S.; Yamakoshi, Y. *J. Am. Chem. Soc.* **2012**, *134*, 20242.

(26) (a) Braida, B.; Walter, C.; Engels, B.; Hiberty, P. C. *J. Am. Chem. Soc.* **2010**, *132*, 7631. (b) Ess, D. H.; Houk, K. N. T. *J. Am. Chem. Soc.* **2007**, *129*, 10646.

(27) Tsuchiya, T.; Rudolf, M.; Wolfrum, S.; Radhakrishnan, S. G.; Aoyama, R.; Yokosawa, Y.; Oshima, A.; Akasaka, T.; Nagase, S.; Guldi, D. M. *Chem- Eur. J.* **2013**, *19*, 557.

(28) Barton, D. H. R.; Doller, D. *Acc. Chem. Res.* **1992**, *25*, 504.

**Scheme 1.** Synthesis of the La@$C_s$-$C_{82}$ derivatives

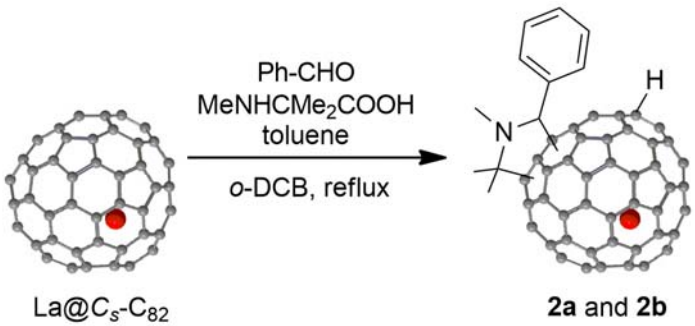

**Scheme 2.** Formation of **2b**-O

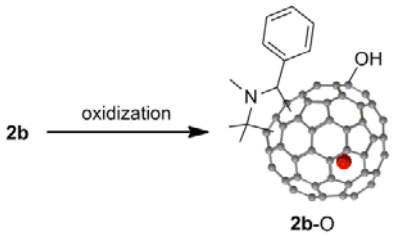


**Scheme 3.** The two possible pathways for the formation of **2**. (Path A) The hydrogen addition following the cycloaddition of azomethine ylide, and (Path B) the inverse sequence.

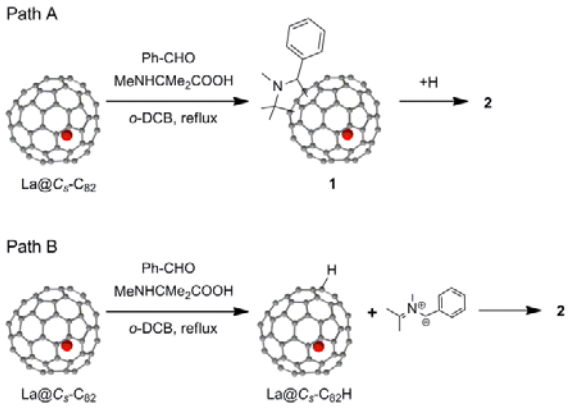


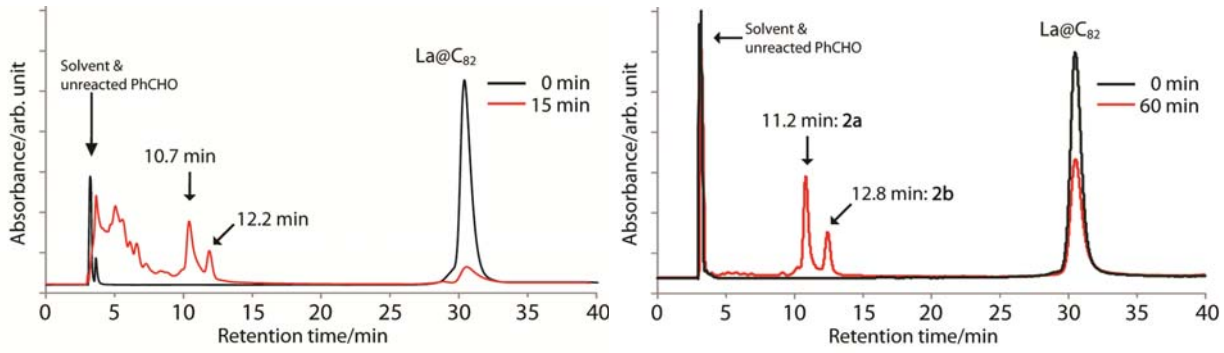


**Figure 1.** HPLC profiles of the 1,3-dipolar cycloaddition (left) without and (right) with the addition of droplet of toluene. The latter reaction afforded **2a** and **2b** selectively. Conditions: Buckyprep column ($\phi$ 4.6 × 250 mm); eluent, toluene; flow rate, 1.0 mL/min; wavelength, 330 nm; temperature, 40 $^{o}$C.

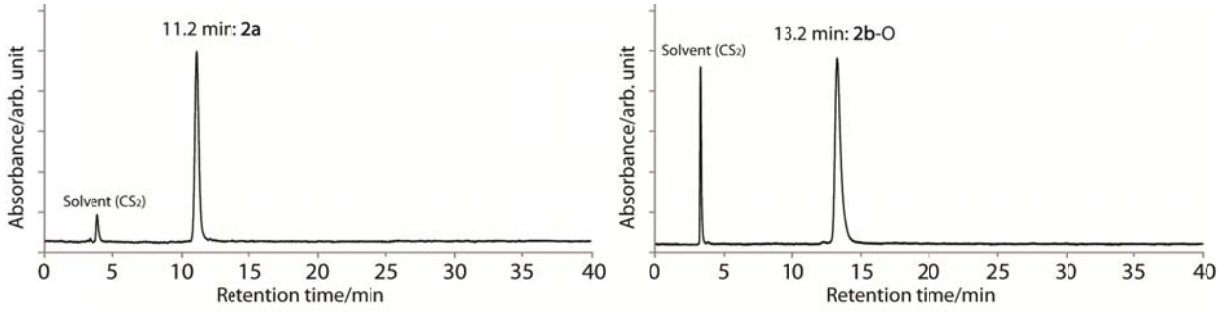


**Figure 2.** HPLC profiles of isolated (left) **2a** and (right) **2b**-O. Conditions: Buckyprep column ($\phi$ 4.6 × 250 mm); eluent, toluene; flow rate, 1.0 mL/min; wavelength, 330 nm; temperature, 40 $^{o}$C.

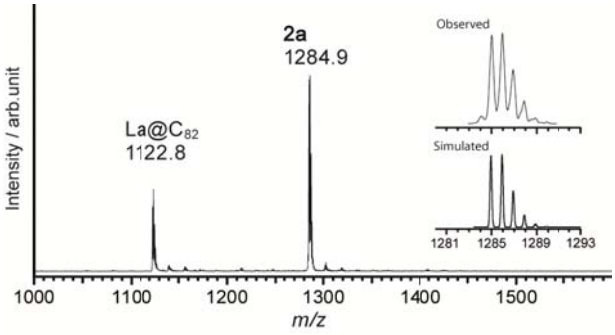


**Figure 3.** MALDI-TOF mass spectra of **2a** accompanied by its magnified view and simulated spectra for **2a**, in negative liner mode using 1,1,4,4-tetraphenyl-1,3-butadiene as a matrix.

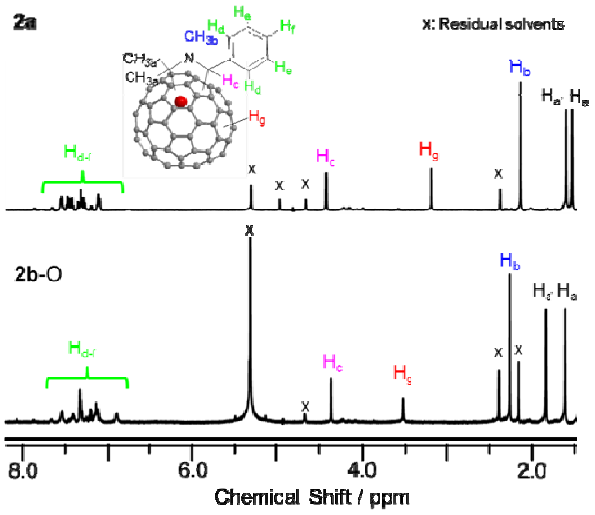


**Figure 4.** $^{1}$H-NMR spectra of **2a** and **2b**-O in $CS_2/CD_2Cl_2$ = 3/1 (v/v).

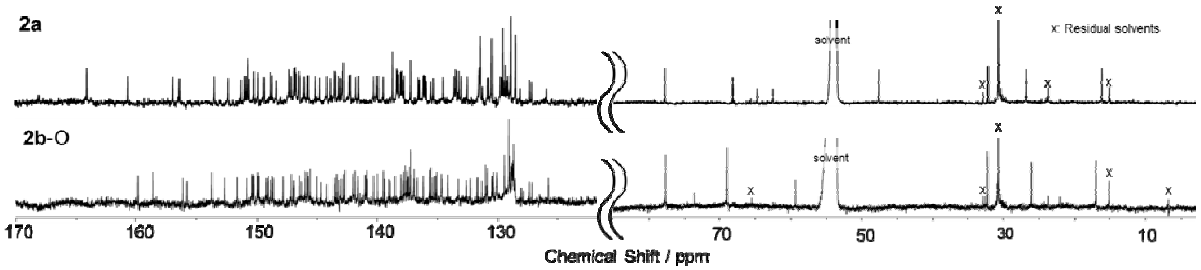


**Figure 5.** $^{13}$C-NMR spectra of **2a** and **2b**-O in $CS_2/CD_2Cl_2$ = 3/1 (v/v).

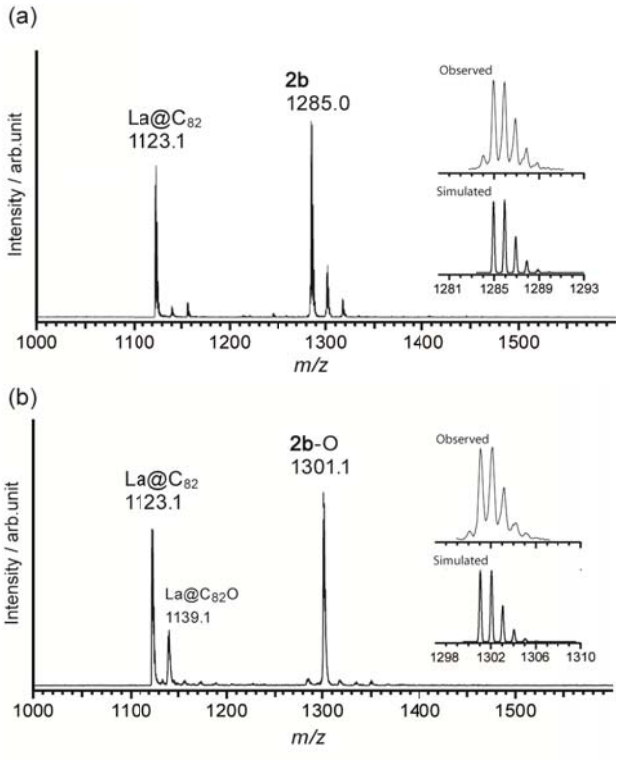


**Figure 6.** MALDI-TOF mass spectra of (a) **2b** which was isolated and measured just after the reaction and (b) isolated **2b**-O, in negative liner mode using 1,1,4,4-tetraphenyl-1,3-butadiene as a matrix.

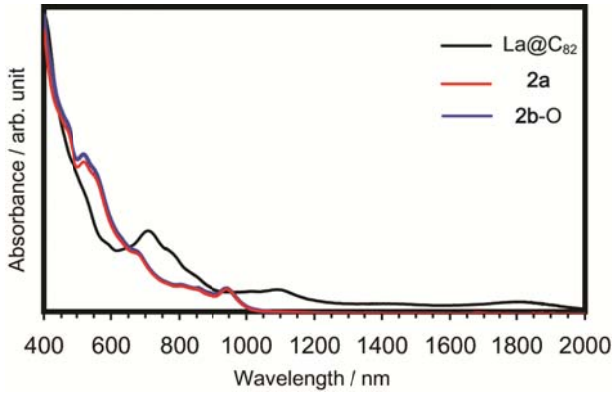


**Figure 7.** UV-vis-NIR spectra of La@$C_s$-$C_{82}$, **2a** and **2b**-O in $CS_2$.

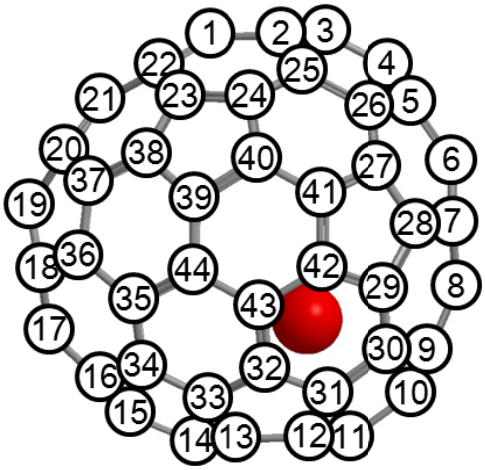


**Figure 8.** Schematic drawing and the numbering of La@$C_s$-$C_{82}$.

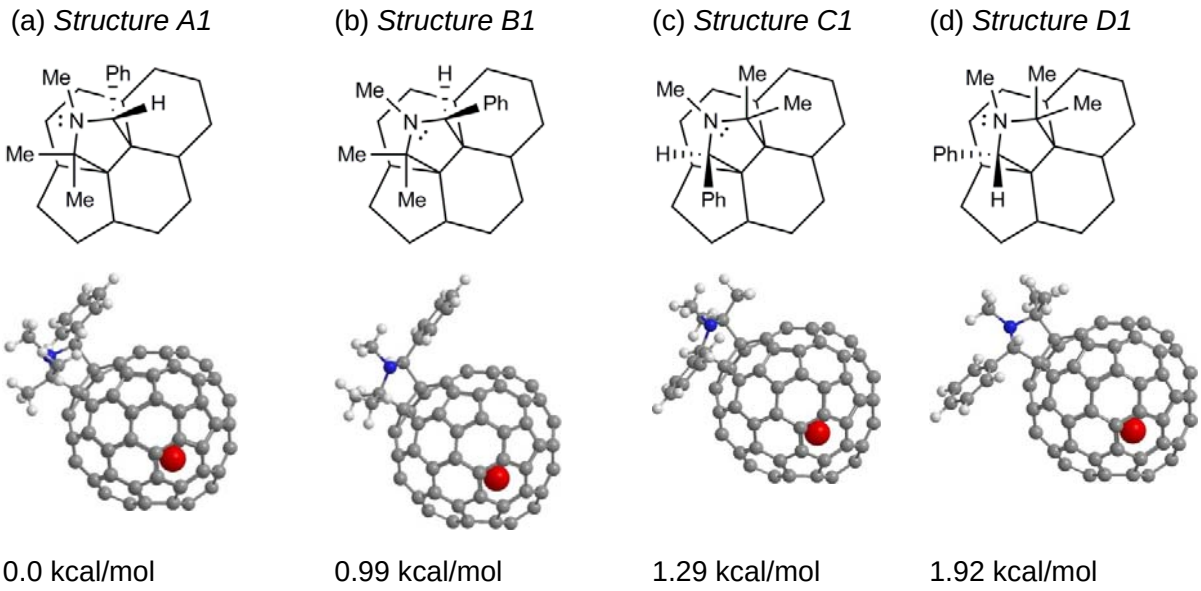


**Figure 9.** Four possible structures of the intermediate **1** based on the first criterion in which the LUMO distribution of dipolarophile is important. The addition site is on C20-C21. They were optimized at the M06-2X/3-21G [C, H, N], SDD [La] level of theory. The numbers in kcal/mol indicate their M06-2X/6-31G* [C, H, N], SDD [La] relative energies of formation.

(a) *Structure A'1* (b) *Structure B'1*

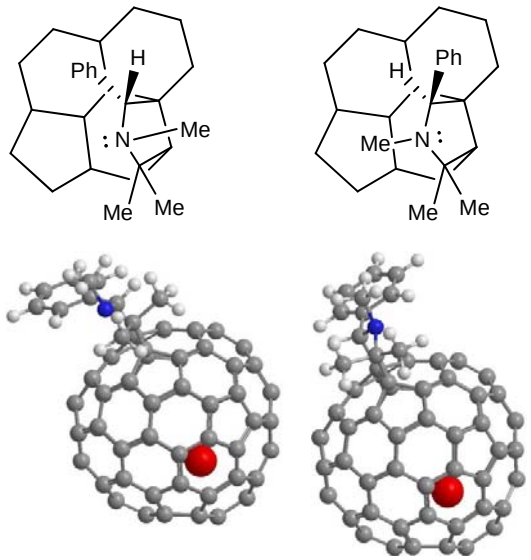


8.81 kcal/mol 9.96 kcal/mol

**Figure 10.** Two possible structures of the intermediate **1** based on the second criterion in which the radical character of azomethine ylide is important. The addition site is on C22-C23. They were optimized at the M06-2X/3-21G [C, H, N], SDD [La] level of theory. The numbers in kcal/mol indicate their M06-2X/6-31G* [C, H, N], SDD [La] relative energies of formation in comparison with *Structure A1* in Figure 8.

*Structure A'1*+ $H_{C3}$ *Structure B'1*+ $H_{C3}$

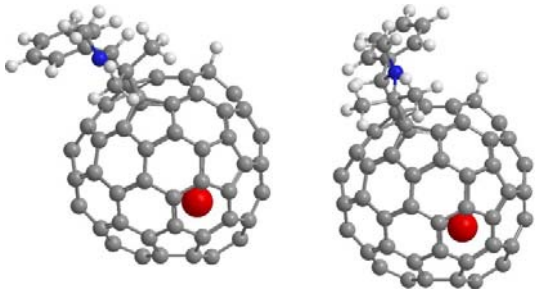

0.00 kcal/mol 0.85 kcal/mol

**Figure 11.** The two most feasible structures for **2** optimized at the M06-2X/3-21G[C, H, N], SDD [La] level of theory. The numbers in kcal/mol indicate their M06-2X/6-31G* [C, H, N], SDD [La] relative energies of formation

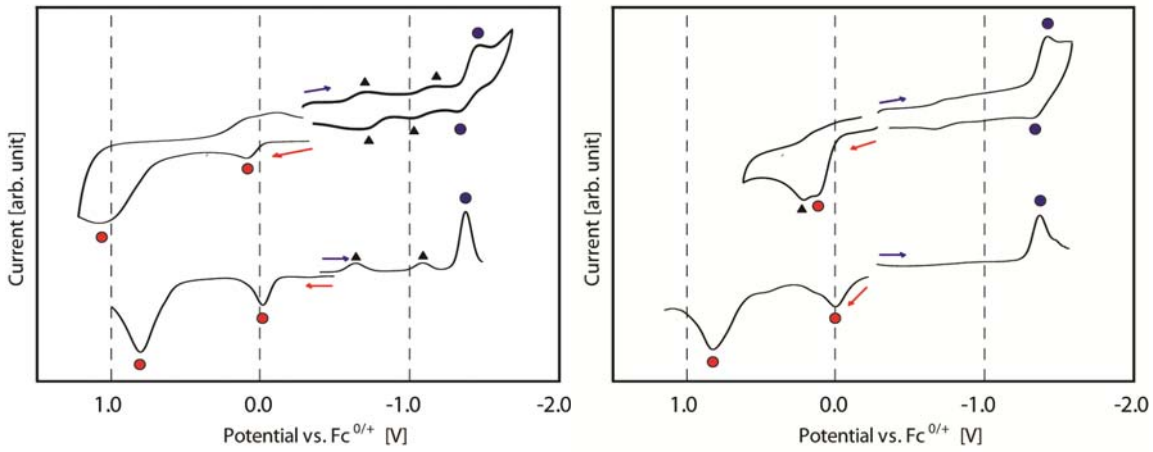


**Figure 12.** CV (upper) and DPV (lower) of **2a** (left) and **2b**-O (right) measured in 0.1 M $TBAPF_6$ in *o*-dichlorobenzene. Circle and triangle symbols indicate redox peaks and the peaks from the compound generated during measurements, respectively.

**Table 1.** $^1$H NMR chemical shifts of hydrogen atoms directly linked to $C_{60}$ in dihydro[60]fullerene and other hydroalkylated and hydroarylated derivatives of $C_{60}$ compared to **2a**.

| Compound | Shift in ppm | Solvent (v/v) | Ref |
|---|---|---|---|
| **2a** | 3.19 | $CD_2Cl_2/CS_2$ = 1/3 | This work |
| $C_{60}H_2$ | 7.00 | $CDCl_3/CS_2$ = 1/1 | 15e |
| $C_{60}HCN$ | 7.19 | $C_2D_2Cl_4/CS_2$ = 1/1 | 15b |
| $C_{60}H(CH_2Ph)$ | 7.84 | $CDCl_3$ | 15g |
| $C_{60}H(C_4H_7O)$ | 6.61 | $CDCl_3/CS_2$ = 1/1 | 15d |
| $C_{60}H(C_4H_8O)$ | 6.34 | $CDCl_3$ | 15f |
| $C_{60}H(C_2F_5)$ | 5.30 | $CDCl_3$ | 15h |

**Table 2.** The five highest Mulliken charge densities, the five highest spin densities and their POAV values in La@$C_s$-$C_{82}$ calculated at the M06-2X/3-21G [C, H, N], SDD [La] level of theory

| Carbon number | Charge density | POAV value |
|---|---|---|
| C42 | 0.012 | 7.82 |
| C23 | 0.009 | 11.23 |
| C20 | 0.009 | 10.90 |
| C16 | 0.008 | 11.11 |
| C27 | 0.007 | 11.21 |

**Table 3.** The five highest Mulliken atomic spin density values and their POAV values in pristine La@$C_s$-$C_{82}$ and **1** calculated at the M06-2X/3-21G [C, H, N], SDD [La] level of theory. For **1**, carbon numbers with prime indicate each another unequivalent carbon atom which originate from a set of two equivalent carbons because of the symmetrical change in the fullerene cage from $C_s$ to $C_1$.

| La@$C_s$-$C_{82}$ | | | | | Structure A1 | Structure B1 |
|---|---|---|---|---|---|---|
| Carbon number | POAV value | Spin density | Carbon number | POAV value | Spin density | Spin density |
| C3 | 11.14 | 0.090 | C3 | 11.03 | 0.095 | 0.091 |
| C23 | 11.23 | 0.068 | C23 | 11.57 | 0.070 | 0.072 |
| C40 | 11.12 | 0.061 | C23’ | 11.12 | 0.069 | 0.067 |
| C1 | 9.78 | 0.059 | C1 | 9.19 | 0.066 | 0.063 |
| C29 | 9.65 | 0.053 | C1’ | 10.09 | 0.062 | 0.062 |

| | | Structure A’1 | Structure B’1 |
|---|---|---|---|
| Carbon number | POAV value | Spin density | Spin density |
| C3 | 10.82 | 0.135 | 0.123 |
| C5 | 10.58 | 0.105 | 0.099 |
| C6 | 10.54 | 0.068 | 0.072 |
| C23’ | 11.32 | 0.065 | 0.059 |
| C25 | 8.80 | 0.048 | 0.044 |

**Table 4.** The Mulliken charge densities of the adjacent carbon atoms of C23 in La@$C_s$-$C_{82}$ calculated at the M06-2X/3-21G [C, H, N], SDD [La] level of theory.

| Carbon number | Charge density |
|---|---|
| C22 | -0.030 |
| C24 | -0.001 |
| C38 | -0.001 |

**Table 5.** Redox potentials.[a, b]

| compd. | $E_{ox}^{(2)}$ | $E_{ox}^{(1)}$ | $E_{red}^{(1)}$ | $E_{red}^{(2)}$ |
|---|---|---|---|---|
| **2a** | 0.80[c] | -0.02[c] | -1.39 | |
| **2b**-O | 0.80[c] | -0.03[c] | -1.40 | |
| La@$C_s$-$C_{80}$[d] | 1.08 | -0.07 | -0.47 | -1.40 |

[a] Values are given in volts relative to a $Fc^{0/+}$ redox couple and were obtained from DPVs. [b] Conditions: working electrode and counter electrode, platinum wires; reference electrode, SCE; supporting electrolyte, 0.1 M $TBAPF_6$ in *o*-DCB. CV: scan rate, 50 mV $s^{-1}$. DPV: pulse amplitude, 50 mV; scan rate, 20 mV $s^{-1}$. [c] Irreversible. [d] Data from Ref 23.

**TOC graphic**